The combined effect of potassium, sodium and calcium on the formation of alkali-silica reaction products

Zhenguo Shi [a*], Barbara Lothenbach [a,b]

[a] Laboratory for Concrete & Construction Chemistry, Swiss Federal Laboratories for Materials Science and Technology (Empa), 8600 Dübendorf, Switzerland

[b] Department of Structural Engineering, Norwegian University of Science and Technology (NTNU), 7491 Trondheim, Norway

[*] Corresponding author. Laboratory for Concrete & Construction Chemistry, Swiss Federal Laboratories for Materials Science and Technology (Empa), 8600 Dübendorf, Switzerland. E-mail address: zhenguo.shi@empa.ch (Z. Shi).

Abstract:

Both alkalis and calcium play essential roles in the formation of alkali-silica reaction (ASR) products. Investigation of their combined effect helps to better understand the conditions of ASR. In this study, samples with a constant Ca/Si ratio of 0.3 but different K(or Na)/Si and K/Na ratios have been synthesized at 80 °C. Experimental studies and thermodynamic modelling show that a sufficient amount of K or Na is essential to initiate ASR; at low alkali concentrations C-S-H is stabilized instead. However, too high alkaline concentrations (≥ 900 mM at K(or Na)/Si ≥ 1) also favor C-S-H formation and suppress ASR product formation. The results reveal a strong effect of the alkalis (K and/or Na) on calcium concentrations and on the formation of ASR products; a maximum ASR product formation is observed at Na or K concentrations between 200 to 500 mM and at initial Ca/Si ratio between 0.1 and 0.4.

Keywords: alkali-silica reaction; ASR-P1; Na-shlykovite; C-S-H; thermodynamic modelling

1. Introduction

Alkali-silica reaction (ASR) is one of the concrete durability issues causing expansion, cracking, and consequently shortening of the service life of concrete. Based on the chemical composition of the ASR products reported in a number of studies [1][2][3][4], it is clear that the presence of reactive silica, alkalis and some calcium are essential conditions for ASR. In addition to be incorporated into ASR products, both alkalis and calcium can also maintain a high pH of the solution which is necessary for dissolution and structural breakdown of reactive silica. However, under certain conditions, rather calcium-silicate-hydrate (C-S-H) containing some alkalis instead of ASR products forms [5][6]. This underlines the need to further explore more precisely the conditions of ASR or C-S-H formation. Moreover, most of the ASR mitigation approaches are based on the design of starting mixtures, such as by proper use of low alkali cements and/or supplementary cementitious materials (SCMs) during concrete manufacturing [7][2]. Thus a better understanding the formation conditions of ASR products is also significant for the development of new approaches to mitigate ASR in existing concrete structures.

Direct evaluation of the precise conditions for formation of ASR products in concrete is difficult due to the small amount and sizes of the ASR products formed in concrete aggregates. ASR products have been recently successfully synthesized in the laboratory [4], which makes it feasible to further investigate the formation conditions of ASR products in such model systems. In a parallel study, the effect of initial Ca/Si ratio on formation of ASR products has been investigated [8]. Both experimental studies and thermodynamic modelling have demonstrated that three different types of ASR products (K-shlykovite: $KCaSi_4O_8(OH)_3 \cdot 2H_2O$, Na-shlykovite: $NaCaSi_4O_8(OH)_3 \cdot 2.3H_2O$, and ASR-P1: $K_{0.52}Ca_{1.16}Si_4O_8(OH)_{2.84} \cdot 1.5H_2O$) could form depending on the initial Ca/Si ratios and type of alkalis. The results showed that all types of the ASR products tend to be converted to C-S-H at Ca/Si ratios over 0.5. More specifically, for the K-containing samples, conversion of the crystalline K-shlykovite to the nano-crystalline ASR-P1 and further to C-S-H was observed with increasing Ca/Si ratios.

In addition to calcium [4][9][10][7][8], also alkalis are essential to form ASR products, since ASR will not form in the absence of alkalis even if calcium hydroxide could also maintain the high level of pH. Small amounts of alkalis do not necessarily lead to the formation of ASR products as alkalis can be incorporated into C-S-H without damaging its intrinsic structure [5][6]. Only few studies determined the minimum OH^- ion concentrations of the pore solution (0.2 – 0.25 M) required to initiate and sustain ASR in concrete [11][12]. Because of the slow formation of ASR products, accelerated testing methods by boosting the alkali content of cements or exposing the samples to high alkaline solution were usually adopted [2]. However, severe alkali boosting might be problematic as it will mask the role of alkalis from the cements [2]. As a consequence, only very few studies have focused on the ASR in concrete with extensively high alkali content [2][13][14]. Interestingly, these studies have shown that extensively high alkali content tend to reduce the ASR expansion in concrete samples [2] and in the NaOH-activated slag mortars [13][14]. These observations could be related to the reduced calcium concentration at very high pH values, as calcium is essential for the formation of ASR products [10]. Other studies showed that very high alkali concentration and thus very high pH values (> 13) result in C-S-H with high Ca/Si ratios [15][16] without causing ASR.

In addition to the alkali concentration, the type of alkalis may also influence the ASR expansion of concrete, as higher expansion is observed for concrete with a relatively higher fraction of Na than K [17]. In fact, accelerated testing methods usually use NaOH instead of KOH and it was observed that the presence of K or Na resulted in formation of different ASR products, even though they have similar crystal structure [4]. Most of the cements contain a higher proportion of K_2SO_4 than Na_2SO_4 [7].

So far, it is not completely clear which calcium and alkalis concentrations lead to the formation of ASR products or C-S-H. In this study, samples with a constant initial Ca/Si ratio of 0.3 but different K(or Na)/Si and K/Na ratios are investigated. After synthesis of these samples at 80 °C, both solid and aqueous phases were analyzed with different techniques. Thermodynamic modeling using the developed thermodynamic data for three different ASR

products i.e., K-shlykovite, Na-shlykovite and ASR-P1 from [8], is also employed to calculate the aqueous compositions and solid phase assemblages. Although the samples were synthesized at high temperature, previous studies have shown strong similarity in term of chemical composition and structure between the synthesized ASR products and ASR products formed in concrete aggregates [4][18], in particular that the synthesized K-shlykovite was almost identical to ASR products formed in concrete aggregate after concrete prism test at 60 °C according to Raman spectroscopy results [4], which support the use of the synthesized ASR products for further understanding ASR.

2. Materials and methods

2.1 Sample preparations

Samples with a constant Ca/Si molar ratio of 0.3 but different K(or Na)/Si and K/Na molar ratios were synthesized by mixing appropriate quantities of SiO_2 (hydrophilic silica, surface area 200 m^2/g, from EVONIK industries) with CaO (obtained by burning calcium carbonate for 12 h at 1000 °C) and analytical KOH (≥ 85% KOH basis, 92 ± 3% based on IC measurements) and/or NaOH (≥ 99.9% NaOH basis) pellet as shown in Table 1 and Fig. 1. For the samples containing only K as alkali source, two series of experiments with high (60 – 100 g per mixing) and low (30 – 50 g per mixing) water contents were prepared. For each series of experiments containing either K or Na as the only alkali source, the water content was somewhat increased for the samples with lower alkali/Si ratios in order to better disperse the solids during mixing. For the samples containing both K and Na, same amount of water was applied, as they have the same (K+Na)/Si molar ratio of 0.5.

All the samples were mixed in 100 mL hard polyethylene (PE-HD) bottles (from Semadeni AG) and equilibrated at 80 °C for 90 days. Afterwards, samples were filtrated using paper filters with mesh size of 20 µm. Roughly 5 mL solution was immediately filtered with 0.45 µm syringe filter for pH measurements and analysis of the solution compositions. The solids were rinsed first with approximately 50 mL of 1:1 water-ethanol solution and then with 50 mL 94% ethanol solution in the N_2 filled glove box. The obtained solids were then

vacuumed dried for 7 days, and stored in N_2 filled desiccators with CO_2 absorbent to minimize carbonation.

2.2 Methods

2.2.1 Experimental methods

The obtained solids were analyzed by a X-ray powder diffraction (XRD, PANalytical X'pert Pro) with CoKα radiation in a θ–θ configuration. The samples were scanned with a step size of 0.017° 2θ between 5 and 90° 2θ with the X'Celerator detector during 150 min. The ^{29}Si MAS NMR spectra were recorded from two laboratories on a Bruker Avance III 400 MHz (9.39T) spectrometer at 79.5 MHz at Empa in Switzerland, and on a Varian Direct-Drive VNMR-600 (14.09 T) spectrometer at 119.1 MHz at Aarhus University in Denmark, using a home-built CP/MAS probes for 7 mm o.d. PSZ rotors. For the 400 MHz NMR spectrometer, the following parameters were applied: 4500 Hz sample rotation rate, minimum of 10240 scans or more, 30° ^{1}H pulse of 2.5 μs, 20 s relaxation delays, RF field strength of 33.3 kHz during SPINAL64 proton decoupling. For the 600 MHz NMR spectrometer, a spinning speed of 6.0 kHz, a 3.0 μs excitation pulse for $\gamma B_1/ 2\pi \approx 42$ kHz, a 60 s relaxation delay, and 2048 scans were employed. The ^{29}Si isotropic chemical shifts are reported relative to neat tetramethyl silane.

The pH was measured for part of the filtrated solution at room temperature around 23 ^{o}C with a Knick pH meter (pH-Meter 766) equipped with a Knick SE100 electrode. The electrode was calibrated with KOH or NaOH solutions of known concentrations to minimize the alkali error caused by the presence of high K and Na concentrations [19]. Another part of filtrated solution was diluted in ratios of 1:10, 1:100 and 1:1000 with MilliQ water immediately after filtration and used for ionic chromatography (IC) analysis. The bulk chemical composition of the obtained solids is calculated by mass balance based on the chemical composition of the starting materials and the chemical composition of the solution at equilibrium by taking into account the bound water in the solids (wt.% of sample ignited at 980°C) measured by thermogravimetric analysis (TGA). For the reported chemical compositions, the impurities of

the KOH pellet used have been taken into account in the mass balance; and the reported errors are calculated by taking into account 10% of analytical error of the measured concentrations used for mass balance.

2.2.2 Thermodynamic modelling

In this study, the PSI/Nagra general thermodynamic database [20] and the Cemdata18 database [21] are used to calculate the ion concentrations in the equilibrium solution and solid phases precipitated. The thermodynamic data for the C-N-S-H [22] and C-K-S-H [8] as summarized in Table 2 are used to predict the precipitation of C-S-H. Experimentally developed thermodynamic data for Na-shlykovite, K-shlykovite and ASR-P1 from another study [8] (see Table 2) are also incorporated in the GEMS codes to predict the formation of ASR products. It should be noted that the general thermodynamic database [20] used describes the aqueous silica complexes at high silica concentration only poorly, in particular at high temperatures as temperature parameters for polynuclear silica species are not available.

3. Results

3.1 Samples containing either K or Na

3.1.1 Phase assemblages

The XRD patterns for the K- or Na-containing samples with high and low water contents after 90 days of reaction are shown in Fig. 2. For K-containing samples, the formation of only C-S-H is observed for the SCK_0 sample without any K as expected, together with some unreacted amorphous silica as reflected by the hump observed at 26° 2θ. In case addition of some K, an amorphous product is observed as the main reaction product for the samples with initial K/Si ratios ranging from 0.25 to 0.75. This phase was recently described by Shi et al. [4] as an nano-crystalline ASR product and named as ASR-P1: $K_{0.52}Ca_{1.16}Si_4O_8(OH)_{2.84}\cdot 1.5H_2O$. According to the previous studies [4][8], a crystalline ASR product (i.e., K-shlykovite: $KCaSi_4O_8(OH)_3\cdot 2H_2O$) could also form in the $CaO\text{-}SiO_2\text{-}K_2O$ system. However, K-shlykovite was only observed for the samples with initial Ca/Si ratios lower than

0.3 [8], which explains the absence of this phase in the present study due to the high Ca/Si ratio of 0.3 used for all the samples. Further increasing K/Si ratio up to 1, ASR-P1 co-existing with C-S-H is observed in the SCK_1 samples with both high and low water contents. The results suggest that a possible destabilization of ASR products to C-S-H can occur at very high alkali content. The opposite, the conversion of C-S-H to ASR products could take place when K/Si ratio is increased from 0 to 0.25 as indicated by the XRD results in Fig. 2.

In contrast to the K-containing samples, where C-S-H is replaced by ASR-P1 at initial K/Si ratio of 0.25, C-S-H remains as the main reaction product when initial Na/Si ratio is up to 0.25 for Na-containing samples. With further increase of Na/Si ratio from 0.5 to 0.75, a crystalline ASR product, Na-shlykovite: $NaCaSi_4O_8(OH)_3 \cdot 2.3H_2O$, is formed as the main reaction product. This phase has been recently identified by Shi et al. [4] to form at 80 °C in the presence of Na and has a similar structure as K-shlykovite. At highest Na/Si ratio of 1, C-S-H is again observed as the main reaction product, indicating a nearly full conversion of Na-shlykovite to C-S-H at high Na content, in contrast to the corresponding K-containing samples where ASR-P1 is only partially converted to C-S-H as shown in Fig. 2. No amorphous ASR product such as ASR-P1 is observed in any of the Na-containing samples.

The formation of ASR-P1 in K-containing samples and Na-shlykovite in Na-containing samples together with formation of C-S-H is also confirmed by ^{29}Si MAS NMR spectra on the selected samples as shown in Fig. 3. For the K-containing samples, the results show that mainly C-S-H with a chemical shift at -85 ppm and some unreacted amorphous silica with a chemical shift at -110 ppm are present in the SCK_0 sample. At higher K/Si ratio of 0.25, the intensity of the Q^2 sites associated with C-S-H is significantly reduced, followed by the increased intensity of Q^3 site with a chemical shift at -91 ppm associated with ASR-P1 according to our previous study [4]. ASR-P1 co-existing with C-S-H is also observed from ^{29}Si NMR spectrum for the $SCK_{0.75}$ sample, although C-S-H is not yet visible from XRD due to the amorphous nature and smaller amount of the C-S-H formed in this sample.

For the Na-containing samples, the ^{29}Si MAS NMR spectra show the presence of mainly low Ca/Si C-S-H and some traces of Q^3 at around 95 ppm from surface Si-OH species of unreacted silica (-110 ppm) in the SCN_0 sample. Minor fraction of Q^2 species related to C-S-H and the dominating Q^3 related to pure Na-shlykovite are observed in the $SCN_{0.5}$ sample, suggesting that a nearly full conversion of C-S-H to Na-shlykovite has taken place by increasing Na/Si ratio up to 0.5. At highest Na/Si ratio of 1, mainly Q^2 associated with C-S-H with traces of Q^3 is observed, suggesting a phase conversion from ASR product to C-S-H. By comparing the ^{29}Si NMR spectra between the samples SCN_0 and SCN_1, around 2-3 ppm chemical shift to less negative values is observed for the SCN_1 sample indicating an uptake of Na in the structure of C-S-H and thus less shielding of the ^{29}Si NMR spectra as reported previously [6][23].

3.1.2 Solution chemistry

The measured concentrations of Ca, K (or Na) and Si in the supernatants together with the pH values measured at 23 °C for the K- or Na-containing samples with high and low water contents are shown in Table 3 and Fig. 4. The results show that the Si concentrations of the equilibrium solution are higher at higher initial K/Si or Na/Si ratios, which is due to the higher K or Na concentrations and thus higher pH values of the solution, as the solubility of amorphous silica is known to increase with the increase of pH [24]. For the two series of K-containing samples with high and with low water contents, the concentration of K and Si are higher for the samples with lower water content. However, no significant differences in the pH values are observed between these two series of experiments as both K and Si concentrations are increased. This effect has been also observed in another study [8]. In contrast to these observations, the calcium concentrations of the equilibrium solutions are one order of magnitude lower for the samples with lower water contents where high Si and K concentrations were present. Moreover, the calcium concentrations decrease with increasing K/Si or Na/Si as a result of the common ion effect between K (or Na), Si and Ca, similar to the tendencies observed for C-(A)-S-H samples in the presence of different quantities of

alkali hydroxide solutions [6][25][26]. This common ion effect indicates the formation of solids, which contain calcium, silicon and potassium.

3.1.3 Thermodynamic modelling

The changes in measured concentrations of the equilibrium solutions and pH values, together with the phase assemblages with increasing K/Si or Na/Si ratio are predicted by thermodynamic modelling as shown in Fig. 5 based on the thermodynamic data for the synthesized ASR products: K-shlykovite, Na-shlykovite and ASR-P1 summarized in Table 2. For comparison, the experimental data from Table 3 are also plotted in the same figure. Generally, thermodynamic modelling shows similar trends for the changes in equilibrium concentrations and pH values with increasing K/Si or Na/Si ratio as the experimental observations. At low K/Si or Na/Si ratios, where ASR-P1 or Na-shlykovite are present, both K (or Na) and Si concentrations increase in parallel, while at higher K/Si or Na/Si ratio (> 0.8) where only C-S-H is predicted, the K or Na concentrations and thus also pH increases while the Si concentrations remains rather constant. For the K-containing samples, the modelled pH values change similarly for the two series samples at high and at low water contents. Some differences in the absolute values between the calculated and measured data were observed, which might be related to poorly described aqueous polynuclear silica complexes at high Si concentrations and at high temperature as already observed in other studies [4][8].

In addition to the equilibrium concentrations, the stable solid phases are also calculated as shown in Fig. 5. The results show that only ASR-P1 is predicted in the K-containing samples for both high and low water contents, which agrees very well with the XRD (Fig. 2) and ^{29}Si NMR (Fig. 3) observations. Na-shlykovite is predicted in the $SCN_{0.5}$ sample, which is also observed from XRD (Fig. 2) and ^{29}Si NMR (Fig. 3) results. The amount of C-S-H is predicted to decrease and then increase with increasing K/Si or Na/Si ratio. The predicted minimum amount of C-S-H is found to be related to the formation of maximum amount of ASR-P1 or Na-shlykovite.

3.1.4 Bulk chemical compositions of the solids

Using the initial compositions of the mixtures and the measured concentrations at equilibrium, the bulk compositions of the solids for the K- or Na-containing samples with both high and low water contents are also calculated by mass balance as summarized in Table 3 and shown in Fig. 6. For comparison, the chemical compositions of the K-shlykovite, ASR-P1 and Na-shlykovite from another study [8] are also plotted in the same figure. The results show that the bulk Ca/Si ratio of the obtained solids increases with the increase of initial K/Si or Na/Si ratio. The observation of higher Ca/Si ratio than those of K-shlykovite, ASR-P1 and Na-shlykovite support the co-precipitation of C-S-H with ASR products observed from experiments and predicted by thermodynamic modelling (Fig. 5). The bulk K/Si ratios for the obtained solids also increase with increasing initial K/Si ratio for the K-containing samples with low water contents, while the bulk K/Si ratio of the obtained solids for the samples with high water contents increases and then decreases with increasing the initial K/Si ratios. The Na/Si ratio of the solids increases first and then tends to be stabilized at Na/Si = 0.25 at very high initial Na/Si ratios. This is also in agreement with the amount of solid phases predicted by thermodynamic modelling in Fig. 5, which is decreasing for ASR products and increasing for C-S-H (similar to K-containing samples). The maximum alkali binding capacity (K or Na) of low C-S-H is about 0.25 [6], comparable to K/Si or Na/Si ratio of 0.25 for Na(K)-shlykovite.

In summary, the Na-containing samples show a similar behavior as the K-containing samples: in both cases ASR products (Na-shlykovite or ASR-P1) are stabilized at intermediate alkali hydroxide concentrations in the range of 200 to 500 mM (see Table 3), while at lower and higher concentrations C-S-H is stabilized instead. The results also show that Na-shlykovite is somewhat less stable than ASR-P1.

3.2 Samples containing both K and Na

3.2.1 Phase assemblages

In addition to the pure K- or Na-containing samples, ASR products with varying combinations of K and Na in difference proportions are also synthesized; all with a total

291 alkali/Si ratio of 0.5; i.e., at conditions where mainly Na-shlykovite or ASR-P1 had formed as
292 discussed above. Their XRD patterns obtained after 90 days of reaction are shown in Fig. 7
293 together with two endmembers ($SCK_{0.5}$ and $SCN_{0.5}$) presented in previous sections. No major
294 differences are observed for all of these samples as ASR-P1 is the only ASR product formed
295 except for the Na-endmember ($SCN_{0.5}$), where Na-shlykovite is present instead. Based on the
296 results in Fig. 2, pure ASR-P1 (e.g. in sample SCK_0) and C-S-H (e.g. in sample $SCK_{0.25}$) can
297 be distinguished by their XRD patterns based on the slight different peak positions. In
298 addition, their XRD patterns between 30 and 35° 2θ also show different line shapes. Pure
299 C-S-H phase synthesized in this study has a narrow and strong asymmetric line shape, while
300 pure ASR-P1 show a broad and nearly symmetric line shape. Thus, the characteristic of both
301 broad and asymmetric line shape for the reaction products formed in the samples containing
302 both K and Na in Fig. 7 indicate the presence of C-S-H in addition to ASR-P1, which is also
303 confirmed by ^{29}Si MAS NMR spectra on the selected samples as shown in Fig. 8. No
304 K-shlykovite is observed in any of the samples, as the relatively high Ca/Si ratio of 0.3 favors
305 the formation of ASR-P1 [4][8]. Na-shlykovite, which is able to form at Ca/Si ratio of 0.3, is
306 not observed in any of the samples containing K, which suggests that the presence of K
307 stabilizes ASR-P1. Overall, the results suggest that ASR-P1 is a quite stable phase, which is
308 able to form at a wide range of K/Na ratios at the investigated temperature of 80 °C.
309
310 **3.2.2 Solution chemistry and thermodynamic modelling**
311 The measured concentrations of Ca, K, Na and Si in the supernatants together with the pH
312 values for the samples containing both K and Na with different K/Na ratios and constant
313 (K+Na)/Si ratio of 0.5 are shown in Table 4 and Fig. 9. As the total alkali concentration
314 (K+Na) is nearly constant, some variation of pH is always accompanied by change of the Si
315 concentration, since the negatively charged silicate ions affect the concentration of OH^- in
316 solution to charge balance Na^+ and/or K^+ ions. Overall, in contrast to the samples containing
317 only K or Na presented in previous sections where the equilibrium concentrations and the
318 measured pH are significantly affected by the initial alkali/Si ratios, the differences in the

measured concentrations and pH values are less significant for all the samples with different K/Na ratios. The similar chemistry environment of the equilibrium solutions supports the XRD observations that mainly one type of ASR products (i.e., ASR-P1) is formed in these samples containing both Na and K.

Thermodynamic modelling for these samples (Fig. 10) also shows that the equilibrium concentrations and pH values are expected to remain more or less constant, which is in line with the experimental results. The main differences between the different samples are the relative concentration of K and Na, which is increasing for K and decreasing for Na with increasing initial K/Na ratios. Both the measured and predicted constant concentration of Si suggests that the dissolved amount of silicon is mainly controlled by the formation of ASR-P1 and thus by the total alkali content and pH. Also some C-S-H is expected to be present in all of the samples. The calculated changes in the K and Na concentrations in the equilibrium solutions agree well with experimentally observed changes. Also the presence of a comparable amount ASR-P1 is predicted for all of these samples as the only type of ASR product, except for the sample with no (or very low) K content.

3.2.3 Bulk chemical compositions of the solids

Based on the initial composition and the measured concentration of the equilibrium solutions, the bulk compositions of the solids for the samples containing both K and Na are calculated by mass balance as summarized in Table 4 and shown in Fig. 11. Generally, the bulk Ca/Si ratios are above 0.3 as shown in Table 4, which are higher than Ca/Si ratio of shlykovite and ASR-P1 without Na, and support the presence of some C-S-H in the samples. The results in Table 4 also show an increase in bulk K/Si ratio and a decrease in Na/Si ratio with increasing initial K/Na ratio. However, the Ca/(K+Na) ratios remain more or less constant except for the $SCK_{0.38}N_{0.12}$ sample.

4. Discussion

The effect of alkali/Si ratio on the formation of ASR products is similar for both K- and Na-containing samples. ASR products form at intermediate alkali contents, while at low and high alkali contents rather C-S-H is stable. At higher initial alkali/Si ratio of 1, ASR products are destabilized to C-S-H, and co-precipitation of ASR product with C-S-H for K-containing sample or formation of only C-S-H in Na-containing is observed. In fact, few studies have demonstrated that ASR expansion could be lowered after extensively boosting the alkalis [2][13][14], in particular for the alkali-activated slag mortars which contain less calcium than Portland cement [13][14]. The present study indicates that the reduced ASR expansion at very high alkali content [2][13][14] is likely due to formation of C-S-H instead of ASR products. The destabilization of ASR products to C-S-H has also been observed in some other studies [3][4][8][27][28] and has been attributed to excess amount of calcium due to the increased initial Ca/Si ratio of the model system [4][8][27], or to the ingress of calcium from its environment in the case of ASR products found near the cement paste of concrete [3][28][18].

The opposite, the conversion of C-S-H to ASR products could take place when alkali/Si ratio is increased from 0 up to over 0.25 as indicated by the XRD results in Fig. 2. Several studies in model systems stated that C-S-H was firstly formed and then converted to ASR products after portlandite was depleted [29][30][27][31]. However, this phenomenon has been so far only identified in model system, where the solutions are initially saturated with portlandite, which may be different from the actual sequence of ASR in concrete. The present study indicates that the formation sequence of ASR products and C-S-H in model system is dependent on the relative amounts of alkalis (K or Na) and of Ca, which can be controlled when mixing the materials in laboratory studies. However, in real concrete K^+ and/or Na^+ ions may enter easier and faster into aggregate due to its smaller radius of hydrated ions compared to the hydrated Ca^{2+} ions [32]. In addition, K^+ and Na^+ concentrations in the pore solution are much higher than Ca concentrations [33][34], which also eases the transport of alkalis into the aggregates. Thus, it is likely that ASR products are firstly formed within the

aggregates in concrete, followed by gradual uptake of calcium and further conversion to C-S-H as evidenced in many studies by the increased Ca/Si of the reaction products away from the center of aggregates [3][28][18]. In addition, it can be expected that the presence of other ions in concrete such as aluminum, lithium as well as the limited availability of water and temperature history would play a further role, indicating the needs of more dedicated and systematic work to reveal the mechanism of ASR.

5. Conclusions

The presence of K and/or Na together with a limited amount of Ca is essential to form ASR products. Different ASR products are formed at 80 °C with different types of alkalis. For the K-containing samples, a nano-crystalline ASR product, ASR-P1 ($K_{0.52}Ca_{1.16}Si_4O_8(OH)_{2.84}\cdot 1.5H_2O$), is observed. In none of the samples is K-shlykovite ($KCaSi_4O_8(OH)_3\cdot 2H_2O$) observed, as the relatively high initial Ca/Si ratio of 0.3 stabilizes rather ASR-P1 than K-shlykovite. In contrast, in the Na-containing samples a crystalline ASR product, Na-shlykovite ($NaCaSi_4O_8(OH)_3\cdot 2.3H_2O$), is formed as Na-shlykovite is slightly more stable than K-shlykovite.

The formation of Na-shlykovite is observed only at Na/Si > 0.25, while in the K-containing systems ASR-P1 is formed at lower K/Si ratios. In the presence of K, ASR-P1 is stabilized instead of Na-shlykovite, such that in all samples containing both K and Na, ASR-P1 is dominant solid formed, indicating that ASR-P1 is more stable than shlykovite at Ca/Si ratios above 0.25 in agreement with our previous observation [8]. Na-shlykovite is observed experimentally only in the absence of K.

Both IC analysis and thermodynamic calculations show that the increase of the initial K(or Na)/Si ratios leads to an increase in pH values and K(or Na) concentrations, but to a reduction in Ca concentrations. As a result, the bulk Ca/Si ratios of the obtained solids increase with increasing initial K(or Na)/Si ratio. In comparison, the increase of the bulk K(or Na)/Si ratio in the obtained solids with increasing the initial K(or Na)/Si ratio is limited and even reduced, for instance for the K-containing samples with high water contents as in

addition to ASR products C-S-H is formed. No obvious changes in solution chemistry and solid compositions are observed for the samples containing both K and Na, as also predicted by thermodynamic modelling.

At a fixed initial Ca/Si ratio of 0.3, ASR products form at intermediate alkali contents, while at low and high alkali contents rather C-S-H and/or amorphous silica are stable. At a fixed alkali/Si ratio of 0.5, ASR products are formed at intermediate Ca/Si ratios from 0.1 to 0.4; at lower Ca/Si ratio SiO_2 is expected to dominate while at higher Ca/Si ratio more C-S-H is present. Together as indicated in Fig. 12, Ca/Si, K/Si and Na/Si ratios at which maximum ASR product formation can be expected.

Acknowledgement

The authors would like to thank the SNF Sinergia: Alkali-silica reaction in concrete (ASR), grant number CRSII5_17108. The EMPAPOSTDOCS-II programme has received funding from the European Union's Horizon 2020 research and innovation programme under the Marie Skłodowska-Curie grant agreement number 754364. Luigi Brunetti and Bin Ma are acknowledged for the IC measurements, and Daniel Rentsch and Jørgen Skibsted for acquiring the ^{29}Si MAS NMR spectra. The thanks are extended to Andreas Leemann and Guoqing Geng for helpful discussions; and to Yiru Yan for analyzing the actual KOH content of the used KOH pellets.

References

[1] A. Leemann, P. Lura, E-modulus of the alkali–silica-reaction product determined by micro-indentation, Constr. Build. Mater. 44 (2013) 221–227.

[2] J. Lindgård, Ö. Andiç-Çakır, I. Fernandes, T.F. Rønning, M.D.A. Thomas, Alkali–silica reactions (ASR): literature review on parameters influencing laboratory performance testing, Cem. Concr. Res. 42 (2012) 223–243.

[3] T. Katayama, ASR gels and their crystalline phases in concrete—universal products in alkali–silica, alkali–silicate and alkali–carbonate reactions, in: Proc. 14th Int. Conf. Alkali Aggreg. React. (ICAAR), Austin, Texas, 2012: pp. 20–25.

[4] Z. Shi, G. Geng, A. Leemann, B. Lothenbach, Synthesis, characterization, and water uptake property of alkali-silica reaction products, Cem. Concr. Res. 121 (2019) 58–71.

[5] S.-Y. Hong, F.P. Glasser, Alkali binding in cement pastes: Part I. The CSH phase, Cem. Concr. Res. 29 (1999) 1893–1903.

[6] E. L'Hôpital, B. Lothenbach, K. Scrivener, D.A. Kulik, Alkali uptake in calcium alumina silicate hydrate (CASH), Cem. Concr. Res. 85 (2016) 122–136.

[7] F. Rajabipour, E. Giannini, C. Dunant, J.H. Ideker, M.D.A. Thomas, Alkali–silica reaction: current understanding of the reaction mechanisms and the knowledge gaps, Cem. Concr. Res. 76 (2015) 130–146.

[8] Z. Shi, B. Lothenbach, The role of calcium on the formation of alkali-silica reaction products, Cem. Concr. Res. (2019) submitted.

[9] R.F. Bleszynski, M.D.A. Thomas, Microstructural studies of alkali-silica reaction in fly ash concrete immersed in alkaline solutions, Adv. Cem. Based Mater. 7 (1998) 66–78.

[10] H. Wang, J.E. Gillott, Mechanism of alkali-silica reaction and the significance of calcium hydroxide, Cem. Concr. Res. 21 (1991) 647–654.

[11] S. Diamond, Effects of Microsilica (Silica Fume) on Pore - Solution Chemistry of Cement Pastes, J. Am. Ceram. Soc. 66 (1983) C–82.

[12] J.J. Kollek, S.P. Varma, C. Zaris, Measurement of OH^- concentrations of pore fluids and expansion due to alkali–silica reaction in composite cement mortars, in: Proc. 8th

448 Int. Cong. Chem. Cem. Rio Janeiro, V.3, Human Kinetics Publishers, 1986: pp. 183–
449 189.
450 [13] Z. Shi, C. Shi, S. Wan, Z. Zhang, Effects of alkali dosage and silicate modulus on
451 alkali-silica reaction in alkali-activated slag mortars, Cem. Concr. Res. 111 (2018) 104–
452 115. doi:10.1016/j.cemconres.2018.06.005.
453 [14] Z. Shi, C. Shi, S. Wan, Z. Ou, Effect of alkali dosage on alkali-silica reaction in sodium
454 hydroxide activated slag mortars, Constr. Build. Mater. 143 (2017) 16–23.
455 [15] H. Matsuyama, J.F. Young, Effects of pH on precipitation of quasi-crystalline calcium
456 silicate hydrate in aqueous solution, Adv. Cem. Res. 12 (2000) 29–33.
457 [16] A. Kumar, B.J. Walder, A. Kunhi Mohamed, A. Hofstetter, B. Srinivasan, A.J. Rossini,
458 K. Scrivener, L. Emsley, P. Bowen, The atomic-level structure of cementitious calcium
459 silicate hydrate, J. Phys. Chem. C. 121 (2017) 17188–17196.
460 [17] A. Leemann, B. Lothenbach, The influence of potassium–sodium ratio in cement on
461 concrete expansion due to alkali-aggregate reaction, Cem. Concr. Res. 38 (2008) 1162–
462 1168.
463 [18] G. Geng, Z. Shi, A. Leemann, C. Borca, T. Huthwelker, K. Glazyrin, I. V. Pekov, S.
464 Churakov, B. Lothenbach, R. Dähn, E. Wieland, Atomistic structure of alkali-silica
465 reaction products refined from X-ray diffraction and micro X-ray absorption data, Cem.
466 Concr. Res. (2019) submitted.
467 [19] B. Traynor, H. Uvegi, E. Olivetti, B. Lothenbach, R.. Myers, Methodology for pH
468 measurement in high alkali cementitious systems, Cem. Concr. Res. (2019) submitted.
469 [20] T. Thoenen, W. Hummel, U. Berner, E. Curti, The PSI/Nagra Chemical
470 Thermodynamic Database 12/07, PSI report 14-04, Villigen PSI, Switzerland, (2014).
471 [21] B. Lothenbach, D.A. Kulik, T. Matschei, M. Balonis, L. Baquerizo, B. Dilnesa, G.D.
472 Miron, R.J. Myers, Cemdata18: A chemical thermodynamic database for hydrated
473 Portland cements and alkali-activated materials, Cem. Concr. Res. 115 (2019) 472–506.
474 [22] R.J. Myers, S.A. Bernal, J.L. Provis, A thermodynamic model for C-(N-) ASH gel:
475 CNASH_ss. Derivation and validation, Cem. Concr. Res. 66 (2014) 27–47.

476 [23] P. Rejmak, J.S. Dolado, M.J. Stott, A. Ayuela, 29Si NMR in cement: a theoretical study
477 on calcium silicate hydrates, J. Phys. Chem. C. 116 (2012) 9755–9761.
478 [24] S. Sjöberg, L.O. Ohman, N. Ingri, Equilibrium and structural studies of silicon (IV) and
479 aluminium (III) in aqueous solution. 11. Polysilicate formation in alkaline aqueous
480 solution. A combined potentiometric and 29 Si NMR study, Acta Chem. Scand. A. 39
481 (1985) 93–107.
482 [25] D.E. Macphee, K. Luke, F.P. Glasser, E.E. Lachowski, Solubility and aging of calcium
483 silicate hydrates in alkaline solutions at 25 C, J. Am. Ceram. Soc. 72 (1989) 646–654.
484 [26] E. L'Hôpital, B. Lothenbach, G. Le Saout, D. Kulik, K. Scrivener, Incorporation of
485 aluminium in calcium-silicate-hydrates, Cem. Concr. Res. 75 (2015) 91–103.
486 [27] X. Hou, L.J. Struble, R.J. Kirkpatrick, Formation of ASR gel and the roles of CSH and
487 portlandite, Cem. Concr. Res. 34 (2004) 1683–1696.
488 [28] A. Leemann, Raman microscopy of alkali-silica reaction (ASR) products formed in
489 concrete, Cem. Concr. Res. 102 (2017) 41–47.
490 [29] T. Kim, J. Olek, Chemical Sequence and Kinetics of Alkali‐Silica Reaction Part I.
491 Experiments, J. Am. Ceram. Soc. 97 (2014) 2195–2203.
492 [30] T. Kim, J. Olek, Chemical Sequence and Kinetics of Alkali–Silica Reaction Part II. A
493 Thermodynamic Model, J. Am. Ceram. Soc. 97 (2014) 2204–2212.
494 [31] X. Hou, R.J. Kirkpatrick, L.J. Struble, P.J.M. Monteiro, Structural investigations of
495 alkali silicate gels, J. Am. Ceram. Soc. 88 (2005) 943–949.
496 [32] L.B. Railsback, Some fundamentals of mineralogy and geochemistry, On-Line Book,
497 Quoted from Www. Gly. Uga. Edu/Railsback. (2006).
498 [33] B. Lothenbach, F. Winnefeld, Thermodynamic modelling of the hydration of Portland
499 cement, Cem. Concr. Res. 36 (2006) 209–226.
500 [34] A. Vollpracht, B. Lothenbach, R. Snellings, J. Haufe, The pore solution of blended
501 cements: a review, Mater. Struct. 49 (2016) 3341–3367.
502
503

Table 1

Starting materials and mixing proportions for the samples.

Samples	SiO_2	CaO	NaOH	KOH	H_2O [a]	water/solid	Ca/Si	(K+Na)/Si	K/Na
	g	g	g	g	g	g/g	mol/mol		
CaO-SiO_2-K_2O with high(low) water contents									
SCK_0	4	1.12	-	0	100	19.5	0.3	0	-
$SCK_{0.25}$	4	1.12	-	0.94	100(50)	16.5(8.25)	0.3	0.25	-
$SCK_{0.5}$	4	1.12	-	1.87	60(30)	8.6(4.3)	0.3	0.5	-
$SCK_{0.75}$	4	1.12	-	2.8	60(30)	7.6(3.8)	0.3	0.75	-
SCK_1	4	1.12	-	3.74	60(30)	6.8(3.4)	0.3	1	-
CaO-SiO_2-Na_2O with only high water contents									
SCN_0	4	1.12	0	-	100	19.5	0.3	0	-
$SCN_{0.25}$	4	1.12	0.67	-	100	17.3	0.3	0.25	-
$SCN_{0.5}$	4	1.12	1.33	-	60	9.3	0.3	0.5	-
$SCN_{0.75}$	4	1.12	1.99	-	60	8.4	0.3	0.75	-
SCN_1	4	1.12	2.66	-	60	7.7	0.3	1	-
CaO-SiO_2-K_2O-Na_2O									
$SCK_{0.455}N_{0.045}$	4	1.12	0.12	1.69	60	8.6	0.3	0.5	10
$SCK_{0.43}N_{0.07}$	4	1.12	0.19	1.6	60	8.7	0.3	0.5	6
$SCK_{0.38}N_{0.12}$	4	1.12	0.33	1.4	60	8.7	0.3	0.5	3
$SCK_{0.30}N_{0.20}$	4	1.12	0.53	1.12	60	8.8	0.3	0.5	1.5
$SCK_{0.25}N_{0.25}$	4	1.12	0.67	0.93	60	8.9	0.3	0.5	1
$SCK_{0.17}N_{0.33}$	4	1.12	0.88	0.62	60	9.1	0.3	0.5	0.5

[a] Two series of samples were prepared for the K-containing samples with low (30 – 50) and high (60 – 100) water contents.

Table 2.

Solubility products for the C-(N-)K-S-H solid solution and three ASR products at 1 atm.

Phases [a]	Log_{10} K_{S0} [b]	Ref
Solubility products for the C-(N-)K-S-H solid solution at 25 °C		
T2C*: $C_{3/2}S_1H_{5/2}$	-11.6	[22]
T5C*: $C_{5/4}S_{5/4}H_{5/2}$	-10.5	[22]
TobH*: $C_1S_{3/2}H_{5/2}$	-7.9	[22]
INFCN: $C_1N_{5/16}S_{3/2}H_{19/16}$	-10.7	[22]
INFCK: $C_1K_{5/16}S_{3/2}H_{19/16}$	-11.2	[8]
Solubility products for the ASR products at 80 °C		
K-shlykovite: $KCaSi_4O_8(OH)_3 \cdot 2H_2O$	-25.8 ± 2.0 [c]	[8]
ASR-P1: $K_{0.52}Ca_{1.16}Si_4O_8(OH)_{2.84} \cdot 1.5H_2O$	-27.1 ± 1.1 [c]	[8]
Na-shlykovite: $NaCaSi_4O_8(OH)_3 \cdot 2.3H_2O$	-26.5 ± 2.0 [c]	[8]

[a] For the nomenclature of C-(N-)K-S-H, the cement chemistry term is used, i.e., C = CaO, N = Na_2O, K = K_2O, S = SiO_2 and H = H_2O. Extrapolation from 25 to 80°C is done using the tabulated entropy and heat capacity values as detailed in [22] and [8].

[b] The solubility products refer to the solubility with respect to the species SiO_2^0, OH^-, H_2O, Ca^{2+}, K^+ and Na^+.

[c] The solubility product of ASR products refer to: $K_{S0,K-shlykovite} = \{K^+\} \cdot \{Ca^{2+}\} \cdot \{SiO_2^0\}^4 \cdot \{OH^-\}^3 \cdot \{H_2O\}^2$; $K_{S0,Na-shlykovite} = \{Na^+\} \cdot \{Ca^{2+}\} \cdot \{SiO_2^0\}^4 \cdot \{OH^-\}^3 \cdot \{H_2O\}^{2.3}$; $K_{S0,ASR-P1} = \{K^+\}^{0.52} \cdot \{Ca^{2+}\}^{1.16} \cdot \{SiO_2^0\}^4 \cdot \{OH^-\}^{2.84} \cdot \{H_2O\}^{1.5}$.

522 Table 3

523 The measured dissolved concentrations in the equilibrium solutions and compositions of the
524 solids for the K- or Na-containing samples with high and low water contents, together with
525 the phases identified in these samples by XRD and ^{29}Si NMR.

Samples	Si	K	Ca	pH [a]		Ca/Si	K(or Na)/Si	Bound water	Identified phases	Log_{10} K_{S0} [b]
	mM	mM	mM	23 °C	80 °C	Solids (mol/mol)		wt%		ASR-P1
K containing samples with high water contents										
SCK_0	0.9	≤ 0.002	0.98	9.5	8	0.30 ± 0.01	-	14.1	C-S-H	-
$SCK_{0.25}$	6.9	28.1	0.03	10.7	9.2	0.30 ± 0.01	0.19 ± 0.01	10.3	ASR-P1	-25.5
$SCK_{0.5}$	135	228	0.33	12.2	10.7	0.34 ± 0.01	0.31 ± 0.03	13.3	ASR-P1	-26.5
$SCK_{0.75}$	308	553	0.34	13.1	11.7	0.41 ± 0.02	0.32 ± 0.08	15.9	ASR-P1+C-S-H	-28.4
SCK_1	448	983	0.09	13.5	12	0.49 ± 0.04	0.16 ± 0.16	18.9	ASR-P1+C-S-H	-29.9
K-containing samples with low water contents										
$SCK_{0.25}$	38.8	42.3	0.05	10.8	9.3	0.31 ± 0.01	0.21 ± 0.01	12.3	ASR-P1	-24.9
$SCK_{0.5}$	399	421	0.1	12.4	10.9	0.36 ± 0.01	0.36 ± 0.02	15.9	ASR-P1	-27.3
$SCK_{0.75}$	603	922	0.02	13.4	11.9	0.41 ± 0.01	0.44 ±0.07	17.2	ASR-P1	-30.1
SCK_1	858	1446	0.03	13.6	12.2	0.47 ± 0.03	0.54 ± 0.13	18.4	ASR-P1+C-S-H	-30.4
Na-containing samples with low water contents										
SCN_0	3.7	≤ 0.01	1	9.2	7.7	0.30 ± 0.01	0	16.6	C-S-H	-
$SCN_{0.25}$	99	82	0.32	11.1	9.7	0.35 ± 0.01	0.15 ± 0.02	20	C-S-H	-
$SCN_{0.5}$	442	382	0.07	11.7	10.2	0.49 ± 0.04	0.27 ± 0.07	21.3	Na-shlykovite+C-S-H	-26.8
$SCN_{0.75}$	427	632	0.01	12.9	11.4	0.48 ± 0.03	0.31 ± 0.12	22.7	Na-shlykovite	-29.1
SCN_1	659	987	0.02	13.1	11.6	0.71 ± 0.11	0.32 ± 0.29	26	C-S-H	-

526 [a] The pH values have been measured at 23°C and corrected for the effect of temperature on measured
527 pH values by deducing 1.47 pH units to account for the strong decrease of measured pH values at
528 higher temperature of 80 °C even at constant OH^- concentrations.

529 [b] At high total Si concentration, polynuclear Si-species dominate the solution; their speciation and
530 stability at higher temperature is not well known, which associates the obtained solubility products with
531 an increased error. The solubility products of ASR-P1 and Na-shlykovite calculated are added for
532 comparison only.

533

Table 4

The measured dissolved concentrations in the equilibrium solutions and compositions of the solids for the samples containing both K and Na together with the phases identified in these samples by XRD.

Samples	Si	Na	K	Ca	pH_{cal}		Ca/Si	K/Si	Na/Si	Bound water	Identified phases	Log_{10} K_{S0} [b]
	mM	mM	mM	mM	23 °C	80 °C [a]	Solids (mol/mol)			wt%		ASR-P1
$SCK_{0.455}N_{0.045}$	241	17.9	224	0.03	11.9	10.4	0.38 ± 0.01	0.28 ± 0.03	0.04 ± 0.01	16.5	ASR-P1	-27.2
$SCK_{0.43}N_{0.07}$	227	32.2	198	0.11	11.9	10.4	0.38 ± 0.01	0.27 ± 0.03	0.05 ± 0.01	17.1	ASR-P1	-26.6
$SCK_{0.38}N_{0.12}$	400	92	228	0.02	11.6	10.1	0.46 ± 0.03	0.22 ± 0.05	0.07 ± 0.01	16.0	ASR-P1	-27.4
$SCK_{0.30}N_{0.20}$	215	119	110	0.04	12.0	10.6	0.37 ± 0.01	0.22 ± 0.02	0.12 ± 0.01	17.3	ASR-P1	-27.5
$SCK_{0.25}N_{0.25}$	196	149	71.2	0.02	12.1	10.7	0.36 ± 0.01	0.20 ± 0.01	0.14 ± 0.01	16.4	ASR-P1	-28.0
$SCK_{0.17}N_{0.33}$	177	193	19.9	0.04	12.1	10.7	0.36 ± 0.01	0.16 ± 0.01	0.19 ± 0.01	17.6	ASR-P1	-28.0

[a] The pH values have been measured at 23 °C and corrected for the effect of temperature on measured pH values by deducing 1.47 pH units to account for the strong decrease of measured pH values at higher temperature of 80 °C even at constant OH^- concentrations.

[b] At high total Si concentration, polynuclear Si-species dominate the solution; their speciation and stability at higher temperature is not well known, which associates the obtained solubility products with an increased error. The solubility products of ASR-P1 calculated are thus added for comparison only.

545

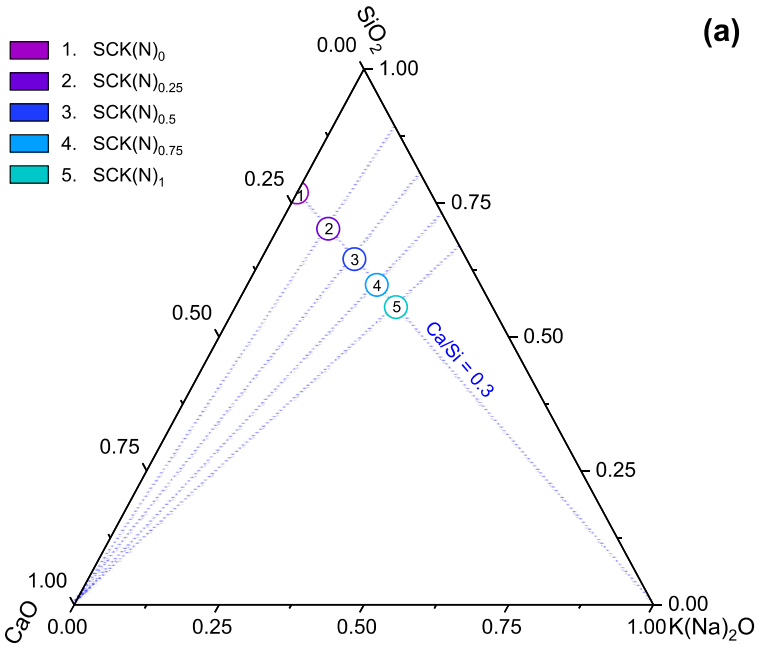

546

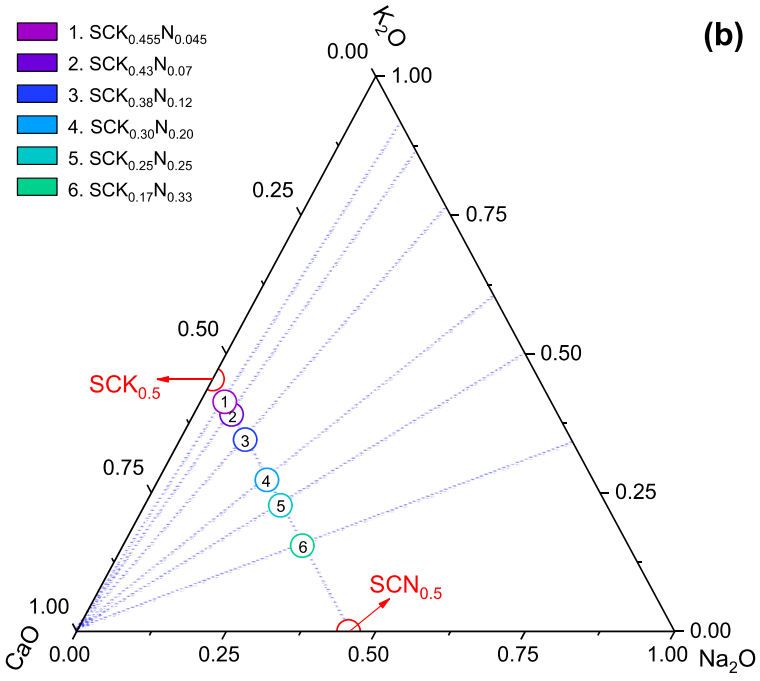

547 Fig. 1. Bulk chemical compositions (units in molar fraction) of the starting materials
548 projected in ternary diagram for (a) the K- or Na-containing samples, and (b) the samples
549 with different K/Na ratios including the two end-members from (a).

550

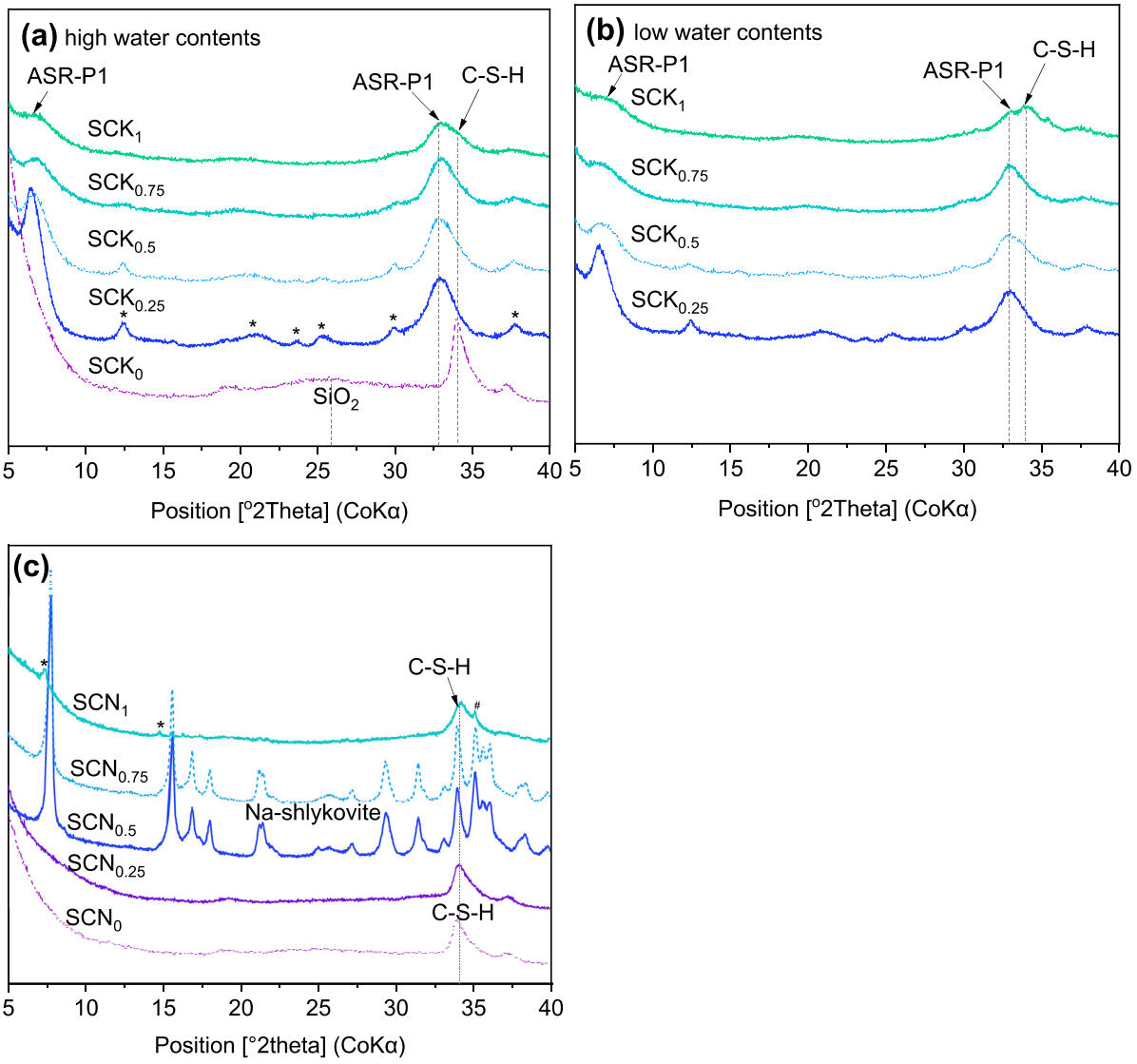

Fig. 2. XRD patterns for the solids obtained after 90 days of reaction for the K-containing samples with (a) high and (b) low water contents, and (c) for the Na-containing samples with high water contents. Note: the asterisk (*) designates the unidentified peaks; the pound sign (#) indicates the presence of natrite (Na_2CO_3, PDF# 98-006-8104) due to a slight carbonation of the alkaline solutions. C-S-H: calcium-silicate-hydrate; ASR-P1: a nano-crystalline ASR product described in [4]. Na-shlykovite is the only crystalline product formed in Na-containing samples with Na/Si ratio of 0.5 and 0.75.

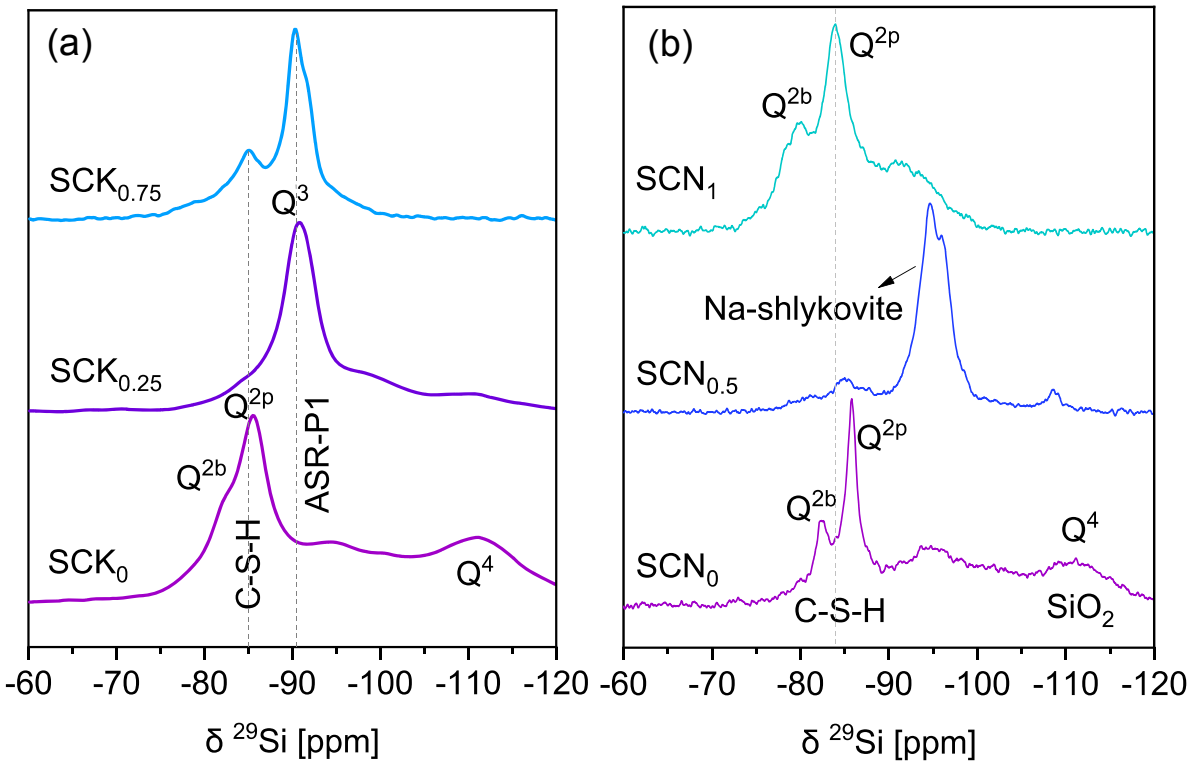

561

562 Fig. 3. ^{29}Si MAS NMR spectra acquired (a) at 79.5 MHz for the selected K-containing
563 samples with high water contents, and (b) at 119.1 MHz for the selected Na-containing
564 samples.

565

566

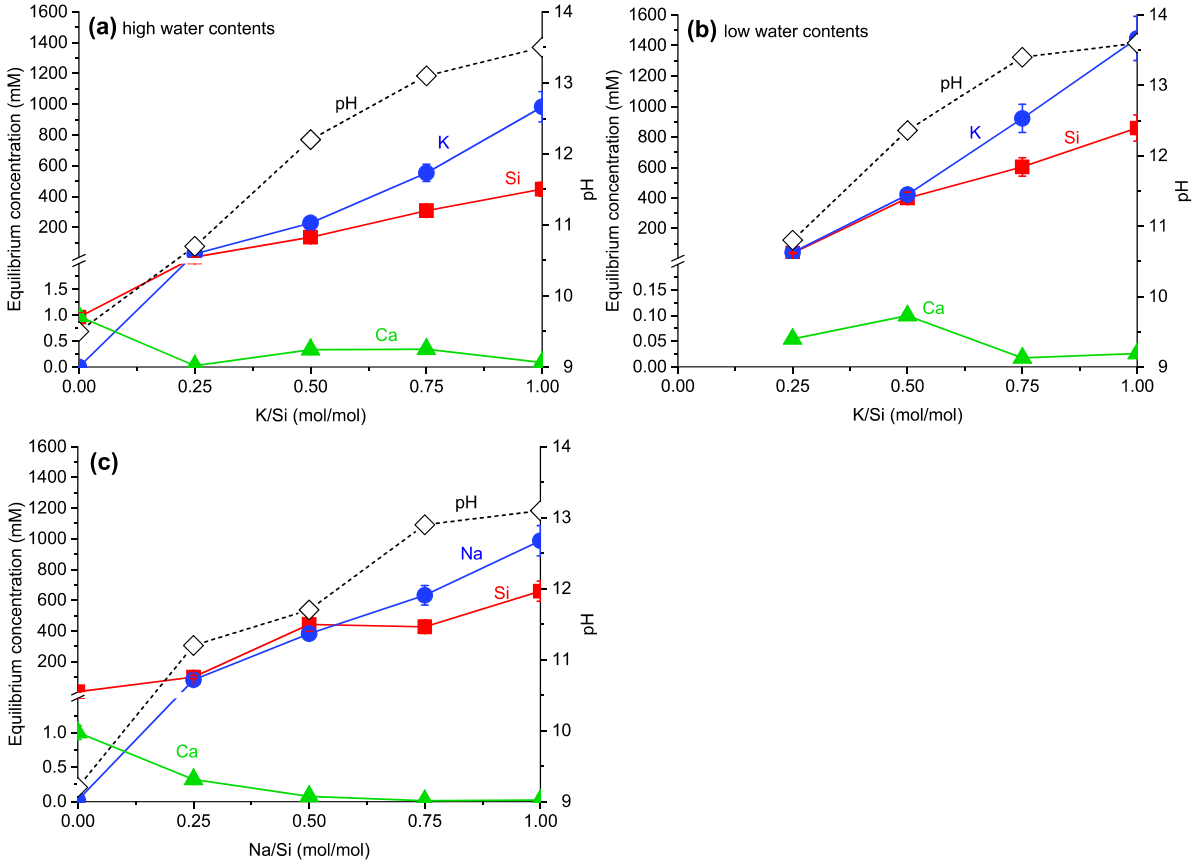

567

568 Fig. 4. Effect of initial alkali/Si ratio on the measured concentrations and pH (measured at
569 23 °C) of the equilibrium solutions for the K-containing samples with (a) high and (b) low
570 water contents, and (c) for the Na-containing samples.

571

572

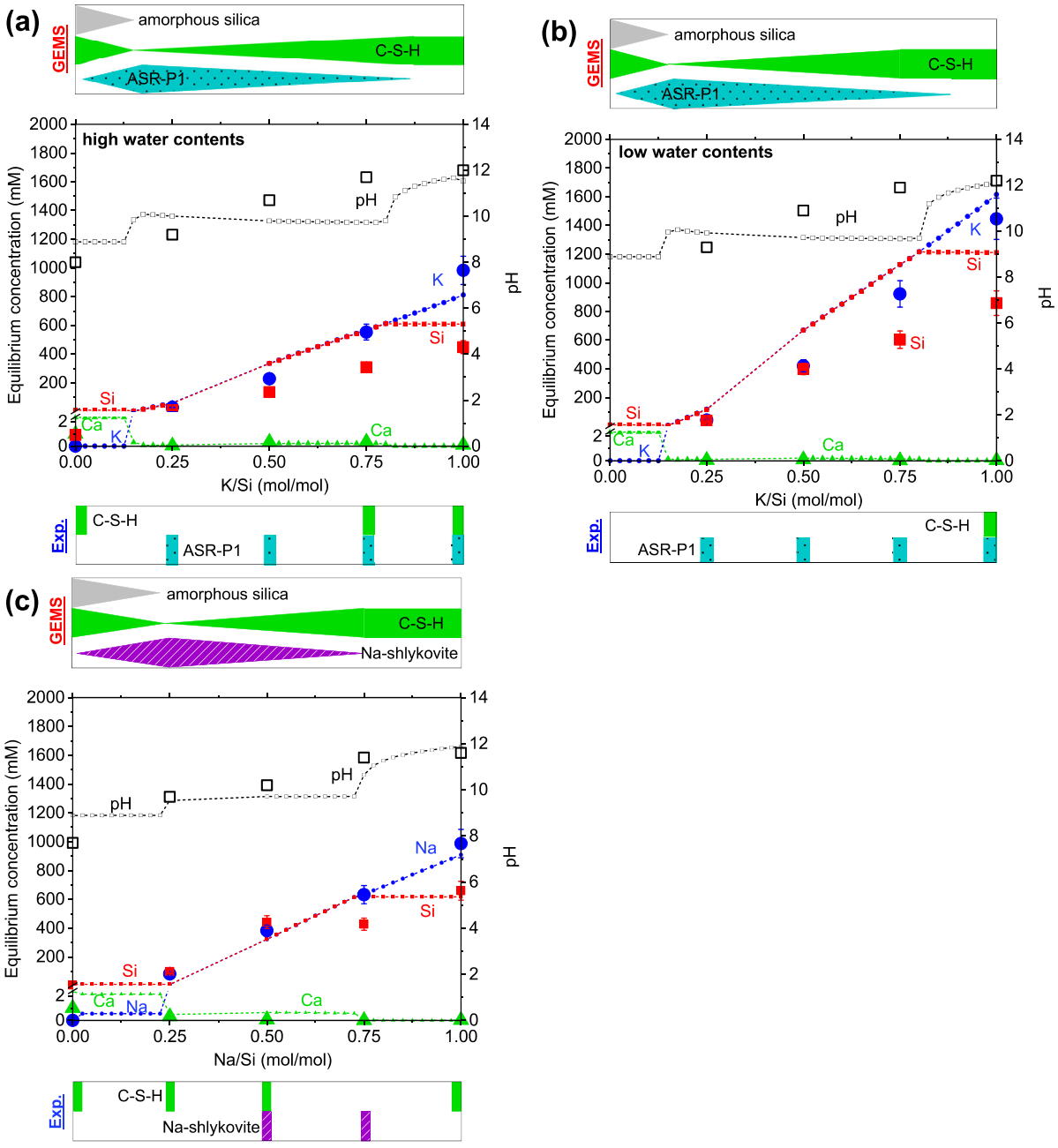

573

574 Fig. 5. Effect of initial K/Si or Na/Si ratio on the solution chemistry and phase assemblages
575 for the K-containing samples with (a) high and (b) low water contents, and (c) Na-containing
576 samples with high water contents at 80 °C. The symbols with smaller size on the dashed lines
577 refer to the data calculated from thermodynamic modelling. No calculations are executed at
578 initial K/Si or Na/Si ratio between 0.25 and 0.5 due to the change of water content. The larger
579 symbols correspond to the experimental data.

580

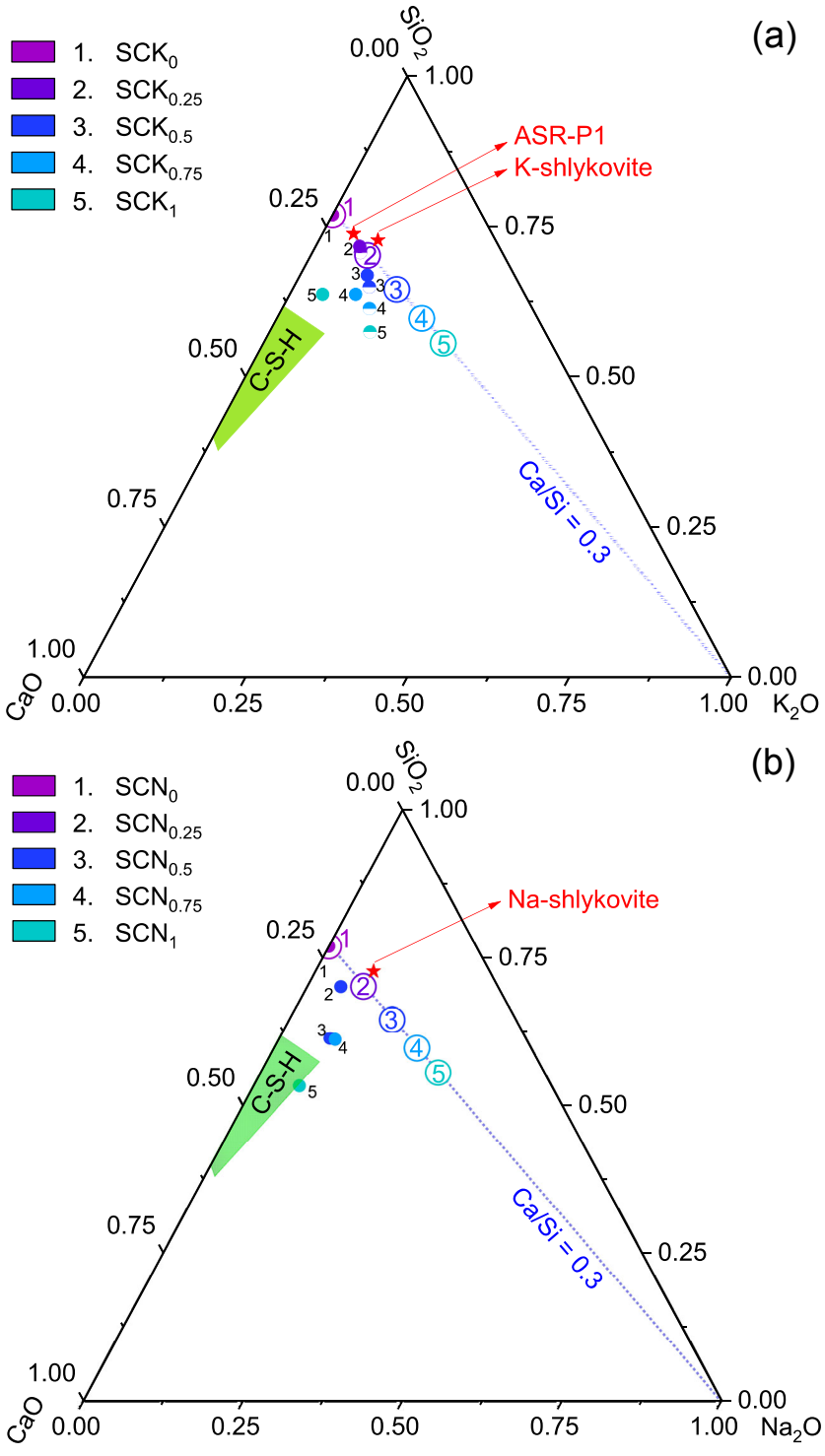

Fig. 6. Bulk chemical compositions (molar fraction) of the staring materials (empty circle) and the solids obtained for the (a) K-containing samples and (b) Na-containing samples after 90 days of reaction at 80 °C (filled circle for the samples with high water contents, and half-filled circle for the samples with low water contents). The chemical compositions for the K-shlykovite, ASR-P1, Na-shlykovite from [8] and the range of C-S-H composition from [6] are also indicated in the diagram.

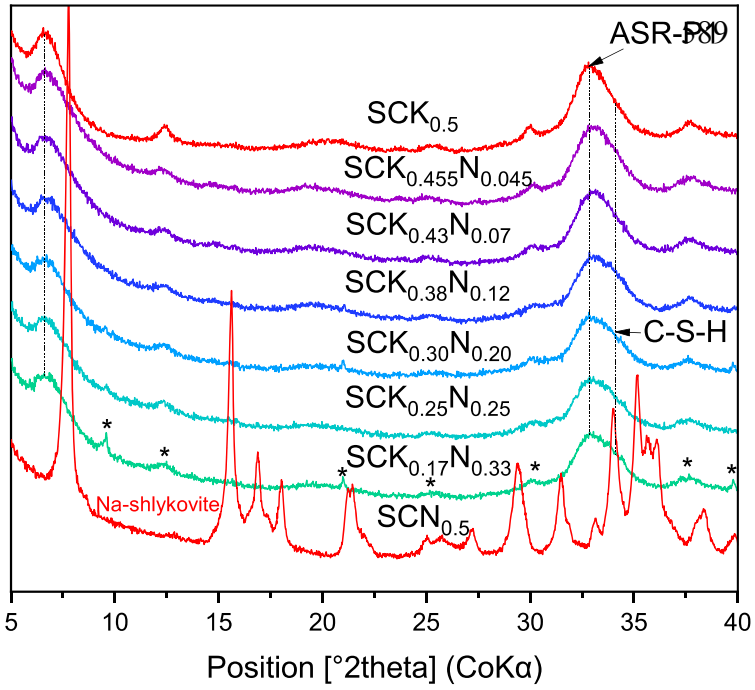

590

591 Fig. 7. XRD patterns of the solids obtained after 90 days of reaction at 80 °C for the samples
592 containing both K and Na with different K/Na ratios indicating the presence of mainly
593 ASR-P1 plus some C-S-H. Two endmembers containing only K ($SCK_{0.5}$) or Na ($SCN_{0.5}$)
594 from previous sections are also plotted in this figure for comparison. Note: the asterisk (*)
595 designates the unidentified peaks.

596

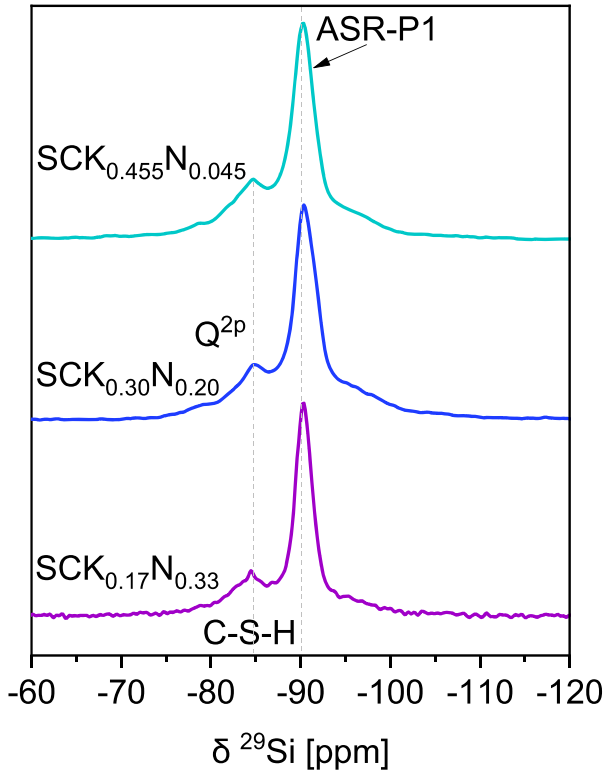

Fig. 8. ^{29}Si MAS NMR spectra acquired at 79.5 MHz for the selected samples containing both K and Na after 90 days of reaction at 80 °C.

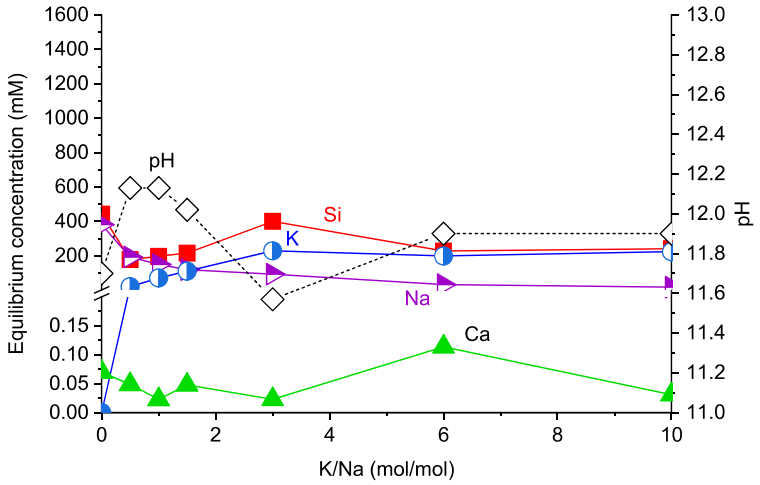

601

602 Fig. 9. Changes of the measured concentrations of the equilibrium solutions together with the
603 measured pH values at 23 °C for the samples containing both K and Na with a constant
604 (K+Na)/Si ratio 0.5 but different K/Na rations. The Na-endmember ($SCN_{0.5}$) with K/Na ratio
605 of 0 from previous section is also plotted in this figure for comparison.

606

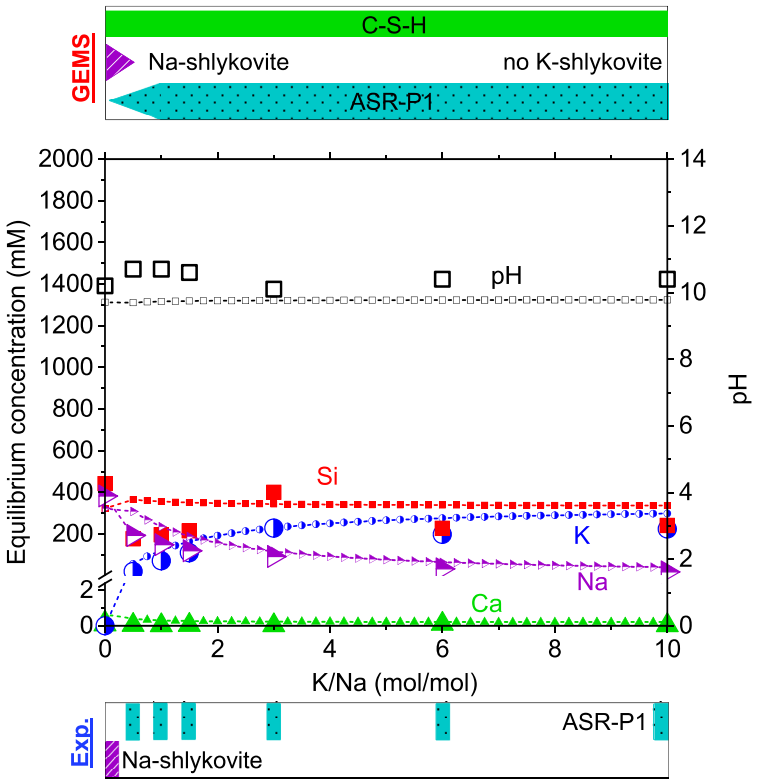

607

608 Fig. 10. Effect of K/Na ratio on the solution chemistry and phase assemblages in the samples
609 containing both K and Na as alkali source. The symbols with smaller size on the dashed lines
610 are data calculated from thermodynamic modelling. The larger symbols correspond to the
611 experimental data. The Na-endmember ($SCN_{0.5}$) with K/Na ratio of 0 from previous section is
612 also plotted in this figure for comparison.

613

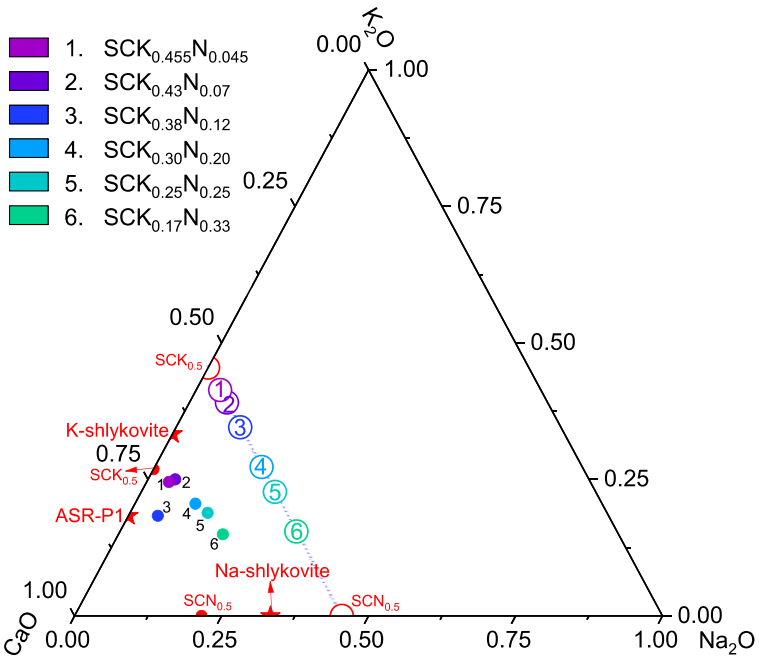

Fig. 11. Bulk chemical compositions (molar fraction) of the staring materials (empty circles) and the solids (filled circles) obtained after 90 days of reaction at 80 °C for the samples containing both K and Na. The chemical compositions for the K-shlykovite, Na-shlykovite and ASR-P1 from [8] are plotted in red star in the diagram. Two endmembers containing only K ($SCK_{0.5}$) or Na ($SCN_{0.5}$) from previous sections are also plotted in this figure for comparison.

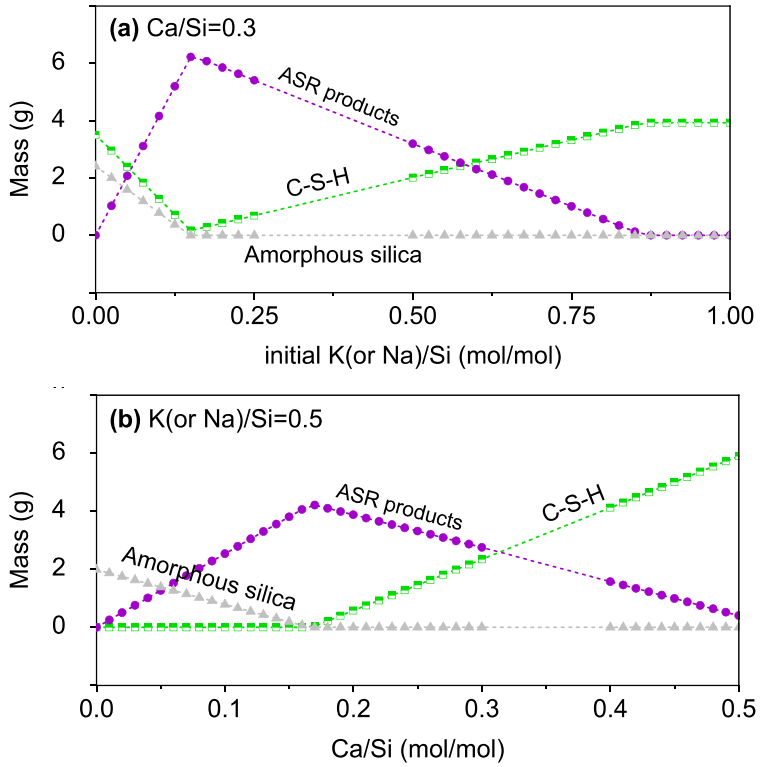

Fig. 12. a) Effect of initial K/Si or Na/Si ratio on the formation of ASR products (ASR-P1 or Na-shlykovite) in the K- or Na-containing samples at a constant initial Ca/Si ratio of 0.3. b) Effect of Ca/Si ratio on formation of ASR products (K-shlykovite, ASR-P1 or Na-shlykovite) in the K- or Na-containing samples at a constant initial K(or Na)/Si ratio of 0.5; reproduced from [8]. The symbols on the dashed lines are data calculated from thermodynamic modelling. No calculations were executed at alkali/Si ratio between 0.25 and 0.5 due to the change of water content.